

# InGaAs-Capped InAs–GaAs Quantum-Dot Infrared Photodetectors Operating in the Long-Wavelength Infrared Range

Wei-Hsun Lin, *Student Member, IEEE*, Chi-Che Tseng, *Student Member, IEEE*, Kuang-Ping Chao, Shu-Cheng Mai, Shih-Yen Lin, *Member, IEEE*, and Meng-Chyi Wu, *Senior Member, IEEE*

**Abstract**—A ten-period InAs–GaAs quantum-dot infrared photodetector (QDIP) with 8-nm  $\text{In}_{0.15}\text{Ga}_{0.85}\text{As}$  capping layer grown after quantum-dot (QD) deposition is investigated. With reduced InAs QD coverage down to 2.0 mono-layers, responses at 10.4 and 8.4  $\mu\text{m}$  are observed for the device under positive and negative biases, respectively. The phenomenon is attributed to the large Stark effect resulted from the asymmetric band diagrams of the device under different voltage polarities. The demonstration of long-wavelength infrared detections with the simple structures of the InGaAs-capped QDIP is advantageous for the development of multicolor QDIP focal-plane arrays.

**Index Terms**—Quantum-dot infrared photodetectors (QDIPs).

## I. INTRODUCTION

MUCH effort has been devoted to the development of quantum-dot infrared photodetectors (QDIPs) [1]–[4]. The influence of different device parameters on the performance of QDIPs has been investigated. QDIPs with high responsivities and high operation temperatures have been reported by inserting AlGaAs barrier layers in the structures to depress dark current [1]–[3]. The influence of quantum-dot (QD) doping density on the operation voltage and normal-incident absorption of the devices has been also reported [4]. The thermal images taken by a  $256 \times 256$  grating-less QDIP focal-plane array (FPA) operated at 135 K have been also demonstrated [5]. However, for most of the QDIPs, the detection wavelengths are limited in the midwavelength infrared [(MWIR) 3–5  $\mu\text{m}$ ] range. To improve this disadvantage, reports with the InAs QDs embedded in InGaAs quantum-well structures (DWELL) have been proposed [6]–[10]. The devices have exhibited the long-wavelength infrared [(LWIR) 8–12  $\mu\text{m}$ ] detection. Large-format FPAs based

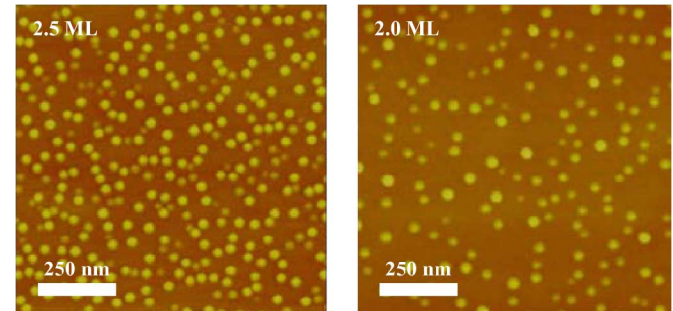


Fig. 1. AFM images of 2.5 and 2.0 ML InAs QDs.

on the devices have demonstrated enhanced wafer uniformity of DWELL samples compared with QDIP samples.

However, for such devices, an additional InGaAs layer prior the QD growth is always required to achieve longer detection wavelengths [10]. With the more complicated structures, device parameter optimization such as underlying InGaAs thickness and growth conditions would be required for high device performances and long detection wavelengths. In this letter, a ten-period InAs–GaAs QDIP with 8-nm  $\text{In}_{0.15}\text{Ga}_{0.85}\text{As}$  capping layer grown after QD deposition is investigated. With reduced InAs QD coverage down to 2.0 mono-layers (ML), responses at 10.4  $\mu\text{m}$  are observed for the device. Due to the smaller QD sizes resulted from the lower coverage, the QD ground state is pushed closer to the quantum-well (QW) ground state in the InGaAs capping layer. In this case, a reduced energy difference between the two states is responsible for the LWIR responses of the device. Also observed for the device is the shorter detection wavelength 8.4  $\mu\text{m}$  under negative biases. The phenomenon is attributed to the large Stark effect resulted from the asymmetric band diagrams of the device.

## II. EXPERIMENTS

The samples discussed in this letter are grown on (100)-oriented semi-insulating GaAs substrates by using the Riber Compact 21 solid-source molecular beam epitaxy system. A ten-period InAs–GaAs QDIP with 8-nm  $\text{In}_{0.15}\text{Ga}_{0.85}\text{As}$  capping layer grown after QD deposition is prepared. After the InGaAs growth, 42-nm undoped GaAs layers are grown as the barriers. The 600- and 300-nm GaAs layers with  $n = 2 \times 10^{18} \text{ cm}^{-3}$  are grown as the bottom and top contact layers. The InAs coverage of the device is 2.0 ML, which is lower than conventional QDIPs. The atomic-force-microscopy (AFM) images of the 2.5 and 2.0 ML InAs QDs are shown in Fig. 1. As show in the figure, dot densities  $3.4 \times 10^{10} \text{ cm}^{-2}$  and  $1.6 \times 10^{10} \text{ cm}^{-2}$

Manuscript received April 24, 2009; revised May 22, 2009. First published July 17, 2009; current version published September 04, 2009. This work was supported in part by the National Science Council, Taiwan under Grant NSC 97-2218-E-002-003 and Grant NSC 97-2623-7-002-003-D.

W.-H. Lin, K.-P. Chao, S.-C. Mai, and M.-C. Wu are with the Institute of Electronics Engineering, National Tsing Hua University, Hsinchu 300, Taiwan (e-mail: twogenius2000@yahoo.com.tw; espn777a@hotmail.com; comanxoxo@msn.com; mcwu@ee.nthu.edu.tw).

C.-C. Tseng is with the Institute of Photonics Technologies, National Tsing Hua University, Hsinchu 300, Taiwan (e-mail: m93530100@gmail.com).

S.-Y. Lin is with the Research Center for Applied Sciences, Academia Sinica, Taipei 11529, Taiwan, the Department of Photonics, National Chiao-Tung University, Hsinchu 300, Taiwan, and the Institute of Optoelectronic Sciences, National Taiwan Ocean University, Keelung 20224, Taiwan (e-mail: shihyen@gate.sinica.edu.tw).

Color versions of one or more of the figures in this letter are available online at <http://ieeexplore.ieee.org>.

Digital Object Identifier 10.1109/LPT.2009.2026630

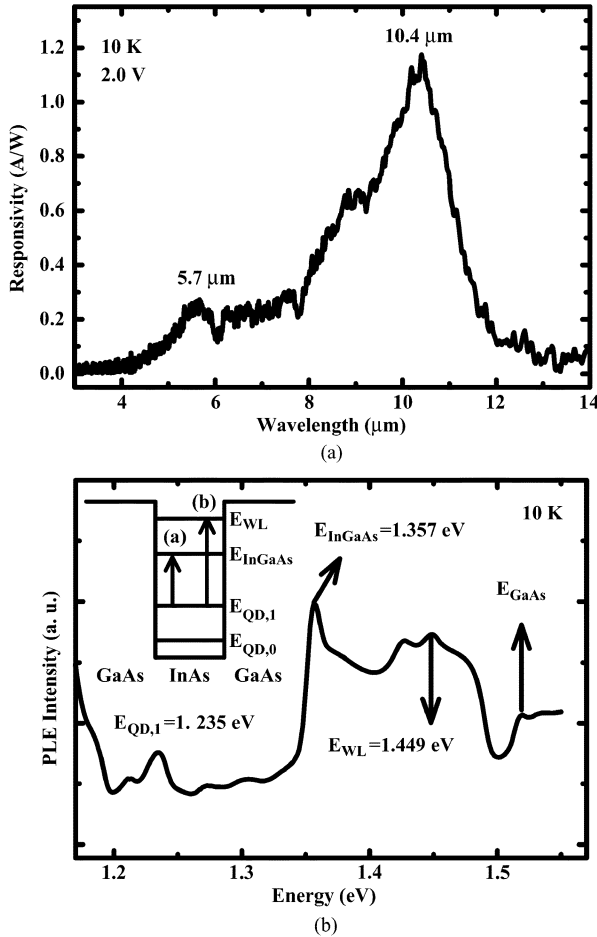


Fig. 2. (a) The 10 K spectral response at 2.0 V and (b) the 10 K PLE spectrum measured at the PL peak energy 1.151 eV of the ten-period InGaAs-capped QDIP. A schematic band diagram of the device is also shown in the inset.

are observed for the 2.5 and 2.0 ML InAs QDs, respectively. Reduced QD average heights from 6.9 to 4.4 nm are also observed with reducing InAs coverage. Standard photolithography and chemical wet etching were adopted to fabricate devices with  $100 \times 100 \mu\text{m}^2$  mesas. Measured under an edge-coupling scheme, the positive and negative biases of the measurements were defined according to the voltages applied to the top contact of the device. The measurement system for spectral response consists of a Perkin Elmer Spectrum 100 Fourier transformation infrared spectroscopy coupling with a Janis cryostat and a current preamplifier [4].

### III. RESULTS AND DISCUSSION

The 2.0-V spectral response of the device is shown in Fig. 2(a). As shown in the figure, peak responses at  $10.4 \mu\text{m}$  with high responsivity 1.2 A/W are observed, while a much weaker peak is observed at  $5.7 \mu\text{m}$ . A high detectivity  $3 \times 10^9 \text{ cm} \cdot \text{Hz}^{1/2}/\text{W}$  is also observed for the device at 2.0 V. The high performances of the device at  $10.4 \mu\text{m}$  suggest high crystalline quality of the sample. Compared with conventional QDIPs, the detection wavelength of the device has been successfully shifted from MWIR to LWIR range [1]–[4]. To explain the transition mechanisms of the device, the 10 K photoluminescence excitation (PLE) spectrum of the sample with its photoluminescence (PL) peak energy 1.151 eV as the

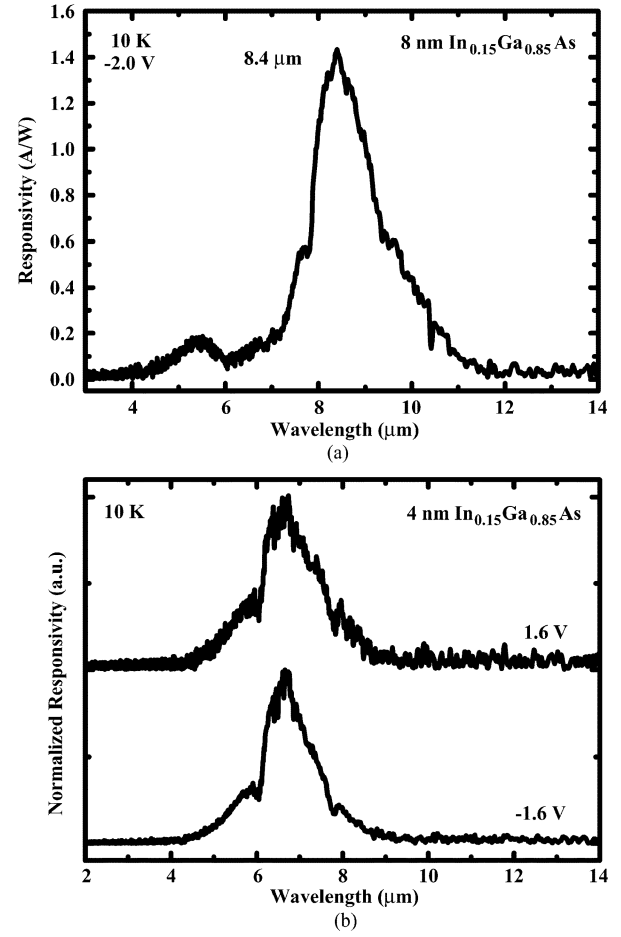


Fig. 3. (a) The 10 K spectral response of the device with 8-nm  $\text{In}_{0.15}\text{Ga}_{0.85}\text{As}$  capping layer at  $-2.0$  V and (b) the normalized 10 K spectral responses of the device with 4-nm  $\text{In}_{0.15}\text{Ga}_{0.85}\text{As}$  capping layer at  $\pm 1.6$  V.

detection wavelength is shown in Fig. 2(b). A schematic band diagram of the device is also shown in the inset. As shown in the figure, four peaks are observed in the PLE spectrum, which are the first excited state of the QDs  $E_{\text{QD},1}$ , the QW ground state in the InGaAs layer  $E_{\text{InGaAs}}$ , the wetting layer state  $E_{\text{WL}}$ , and the GaAs band edge absorption  $E_{\text{GaAs}}$ . Therefore, the main transitions responsible for the spectral response of the device should be (a)  $E_{\text{QD},1} - E_{\text{InGaAs}}$  and (b)  $E_{\text{QD},1} - E_{\text{WL}}$  transitions. The energy differences for the two transitions are 0.122 and 0.214 eV ( $10.16$  and  $5.79 \mu\text{m}$ ), respectively. As shown in Fig. 2(a), both transitions are observed in the spectral responses while the dominant one at 2.0 V is the  $E_{\text{QD},1} - E_{\text{InGaAs}}$  transition.

However, when the device is operated under  $-2.0$  V, the response peak would shift from  $10.4$  to  $8.4 \mu\text{m}$  as shown in Fig. 3(a). A similar phenomenon has also been observed for the DWELL devices [9]. One possible mechanism responsible for this phenomenon is the large Stark shift as described in the step QWs [11]. In that paper, blue (red) Stark shift of the absorption spectrum is observed for the step QWs under negative (positive) biases with similar energy differences. In the case of the current device, the energy difference of  $E_{\text{QD},1} - E_{\text{InGaAs}}$  is 0.122 eV, as shown in Fig. 2(b). When the device is under positive/negative biases, the detection wavelength of the device is  $10.4/8.4 \mu\text{m}$ , which is  $-2.8/25.6$  meV shift from the energy

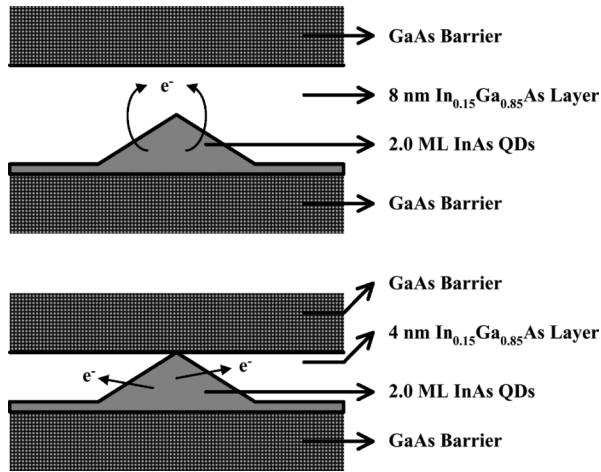


Fig. 4. Schematic cross-sectional diagrams of the devices with 8- and 4-nm  $\text{In}_{0.15}\text{Ga}_{0.85}\text{As}$  capping layers.

difference  $E_{\text{QD},1} - E_{\text{InGaAs}}$  of 0.122 eV. In this case, it seems obvious that the Stark effect should be responsible for the detection wavelength shift under different voltage polarities. However, the other QDIP device with a thinner InGaAs capping layer does not reveal similar results.

The normalized 10 K spectral responses at  $\pm 1.6$  V of the device with similar structure except for the thinner  $\text{In}_{0.15}\text{Ga}_{0.85}\text{As}$  down to 4 nm are shown in Fig. 3(b). As shown in the figure, a shorter detection wavelength  $6.7 \mu\text{m}$  is observed for the device. The phenomenon is attributed to the higher InGaAs QW ground state resulted from the thinner QW thickness. In this case, larger energy difference between the QD excited states and InGaAs state would result in shorter detection wavelengths. Also observed in the figure are the similar detection wavelengths of the device under different voltage polarities. The phenomenon is quite different from the performances of the device with the 8-nm  $\text{In}_{0.15}\text{Ga}_{0.85}\text{As}$  capping layer.

To explain the phenomenon, schematic cross-sectional diagrams of the two devices are shown in Fig. 4. As shown in the figure, for the device with 8-nm  $\text{In}_{0.15}\text{Ga}_{0.85}\text{As}$  capping layers, the capping layer thickness would exceed the average QD height of 4.4 nm. As for the device with 4-nm  $\text{In}_{0.15}\text{Ga}_{0.85}\text{As}$  capping layers, the capping layer would barely cover the InAs QDs. Since the dominate transition for the InGaAs-capped QDIPs is the  $E_{\text{QD},1} - E_{\text{InGaAs}}$  transition, the photo-excited electrons would escape from the InAs QDs to the capping layers. Therefore, for the device with thicker capping layers, the photo-excited electrons would escape from the QDs to the InGaAs layer right above the QD structures since the electrical fields are applied vertically to the heterostructures. In this case, the asymmetric band diagrams of the InGaAs capping layer/InAs QDs embedded in GaAs barriers would result in large Stark shifts. However, for the device with thinner capping layers, the photo-excited electrons would escape from InAs QDs to the neighboring InGaAs capping layers. For the InGaAs layer surrounded the InAs QDs, the band diagrams are similar with a symmetric InGaAs QW with GaAs barriers. In this

case, no significant Stark effect would be observed such that identical detection wavelengths are observed for the device with 4-nm  $\text{In}_{0.15}\text{Ga}_{0.85}\text{As}$  capping layers under positive and negative biases.

#### IV. CONCLUSION

A ten-period InAs–GaAs QDIP with 8-nm  $\text{In}_{0.15}\text{Ga}_{0.85}\text{As}$  capping layer grown after QD deposition is investigated. With reduced InAs QD coverage down to 2.0 ML, responses at  $10.4 \mu\text{m}$  are observed for the device. Also observed for the device is the shorter detection wavelength  $8.4 \mu\text{m}$  under negative biases. Compared with the device with thinner capping layers, the phenomenon is attributed to the large Stark effect resulted from the asymmetric band diagrams of the over-capped InGaAs layer over the 2.0 ML InAs QDs. The demonstration of LWIR response with high performances by using the simple InGaAs-capped QD structures would be advantageous for the application of multicolor QDIP FPAs.

#### REFERENCES

- [1] S. Y. Lin, Y. R. Tsai, and S. C. Lee, "High-performance InAs/GaAs quantum-dot infrared photodetector with single-sided  $\text{Al}_{0.3}\text{Ga}_{0.7}\text{As}$  blocking layer," *Appl. Phys. Lett.*, vol. 78, pp. 2784–2786, Apr. 2001.
- [2] S. Chakrabarti, A. D. Stiff-Roberts, P. Bhattacharya, S. Gunapala, S. Bandara, S. B. Rafol, and S. W. Kennerly, "High-temperature operation of InAs–GaAs quantum-dot infrared photodetectors with large responsivity and detectivity," *IEEE Photon. Technol. Lett.*, vol. 16, no. 5, pp. 1361–1363, May 2004.
- [3] S. F. Tang, S. Y. Lin, and S. C. Lee, "Near-room-temperature operation of an InAs/GaAs quantum-dot infrared photodetector," *Appl. Phys. Lett.*, vol. 78, pp. 2428–2430, Apr. 2001.
- [4] S. T. Chou, M. C. Wu, S. Y. Lin, and J. Y. Chi, "The influence of doping density on the normal incident absorption of quantum-dot infrared photodetectors," *Appl. Phys. Lett.*, vol. 88, pp. 173511–173513, Apr. 2006.
- [5] S. F. Tang, C. D. Chiang, P. K. Weng, Y. T. Gau, J. J. Ruo, S. T. Yang, C. C. Shih, S. Y. Lin, and S. C. Lee, "High-temperature operation normal incident  $256 \times 256$  InAs/GaAs quantum dot infrared photodetector focal plane array," *IEEE Photon. Technol. Lett.*, vol. 18, no. 8, pp. 986–988, Apr. 15, 2006.
- [6] S. D. Gunapala, S. V. Bandara, C. J. Hill, D. Z. Ting, J. K. Liu, S. B. Rafol, E. R. Blazewski, J. M. Mumolo, S. A. Keo, S. Krishna, Y. C. Chang, and C. A. Shott, "Long-wavelength infrared (LWIR) quantum dot infrared photodetector (QDIP) focal plane array," *Proc. SPIE*, vol. 6206, p. 62060J, 2006.
- [7] S. Krishna, D. Forman, S. Annamalai, P. Dowd, P. Varangis, T. Tumulillo, A. Gray, J. Zilko, K. Sun, M. Liu, J. Campbell, and D. Carothers, "Demonstration of a  $320 \times 256$  two-color focal plane array using InAs/InGaAs quantum dots in well detectors," *Appl. Phys. Lett.*, vol. 86, pp. 193501-1–193501-3, May 2005.
- [8] G. Ariyawansa, A. G. Unil Perera, G. S. Raghavan, G. Von Winckel, A. Stintz, and S. Krishna, "Effect of well width on three-color quantum dots-in-a-well infrared detectors," *IEEE Photon. Technol. Lett.*, vol. 17, no. 5, pp. 1064–1066, May 2005.
- [9] L. Höglund, P. O. Holtz, H. Pettersson, C. Asplund, Q. Wang, H. Malm, S. Almqvist, E. Petrini, and J. Y. Andersson, "Bias mediated tuning of the detection wavelength in asymmetrical quantum dots-in-a-well infrared photodetectors," *Appl. Phys. Lett.*, vol. 93, pp. 203512-1–203512-3, Nov. 2008.
- [10] S. Raghavan, D. Forman, P. Hill, N. R. Weisse-Bernstein, G. von Winckel, P. Rotella, S. Krishna, S. W. Kennerly, and J. W. Little, "Normal-incidence InAs/ $\text{In}_{0.15}\text{Ga}_{0.85}\text{As}$  quantum dots-in-a-well detector operating in the long-wave infrared atmospheric window ( $8\text{--}12 \mu\text{m}$ )," *J. Appl. Phys.*, vol. 96, pp. 1036–1039, Jul. 2004.
- [11] Y. J. Mii, P. G. Karunasiri, K. L. Wang, M. Chen, and P. F. Yuh, "Large Stark shifts of the local to global state intersubband transitions in step quantum wells," *Appl. Phys. Lett.*, vol. 56, pp. 1986–1988, May 1990.